

Retraction Notice

The Editor-in-Chief and the publisher have retracted this article, which was submitted as part of a guest-edited special section. An investigation uncovered evidence of systematic manipulation of the publication process, including compromised peer review. The Editor and publisher no longer have confidence in the results and conclusions of the article.

ZL, YY, BJ, and YC did not agree with the retraction.

Automatic reading recognition of pointer barometer based on machine vision

Zuhe Li^{a,b}, Yuan Yu,^{a,*} Baohua Jin,^a and Yuhao Cui^a

^aZhengzhou University of Light Industry, School of Computer and Communication Engineering, Zhengzhou, Henan, China

^bZhengzhou University of Light Industry, Henan Key Laboratory of Food Safety Data Intelligence, Zhengzhou, Henan, China

Abstract. To develop a calibration system for a pointer barometer based on machine vision, an automatic reading recognition scheme of the barometer based on color images is proposed. To locate the dial while extracting the pointer, an optimized three-point-based circle determination method is proposed to calibrate the dial center and segment the dial. At the same time, an improved angle method is proposed to realize the automatic reading recognition of pointer instruments. First, the pointer area is detected and extracted by the three frame difference method, and the pointer centroids are extracted by least circumscribed rectangle fitting, and the optimal three points are selected to determine the center of the circle and locate the dial. Then, the two-color image matrix elements corresponding to different pointers are compared point by point to obtain the maximum value, and the dial without the pointers is also obtained. Through cropping, color channel component extraction, and binarization processing on the dial without pointers, a noninterference dial scale image is refitted, and each scale is fitted with a minimum circumscribed rectangle to calibrate the centroid of the scale line. Finally, using the centroids of the calibrated scale lines, the centroid of the fitted pointer, and the circle center obtained by three-point-based circle determination, the improved angle method proposed is used to realize the automatic reading recognition of the pointer instrument. Experimental results show that this scheme can effectively improve the accuracy of machine vision-based automatic reading recognition for pointer instruments. © 2022 SPIE and IS&T [DOI: 10.1117/1.JEI.31.5.051415]

Keywords: pointer instrument; reading recognition; frame difference; angle method.

Paper 220062SS received Jan. 17, 2022; accepted for publication Apr. 11, 2022; published online Apr. 27, 2022; retracted Jun. 24, 2023.

1 Introduction

Pointer instruments are widely used in power transmission, oil exploitation, aerospace, and other fields because of their simple structure, convenient maintenance, strong ability to withstand electromagnetic interference, high precision, and low price.^{1,2} However, they require a lot of repetitive work during delivery inspection and daily manual reading, especially when performing quality inspection and interpretation of large-scale meters. Time-consuming, repetitive work can easily cause visual fatigue of staff, resulting in large meter reading errors and poor quality inspection.^{3,4}

With the continuous improvement of digital information technology in recent years, a variety of high-quality and high-performance camera equipment has been popularized, which provides an auxiliary means for the verification and detection of traditional analog pointer instruments. For example, an instrument reading recognition system based on computer vision technology can use the superior data processing capabilities of modern computers to automate the detection process⁵⁻⁷ and replace the original manual operation to complete the acquisition, display, storage, and report printing of reading results. This avoids a large number of repetitive manual

*Address all correspondence to Yuan Yu, YuYuan@zzuli.edu.cn

operations and provides an effective method for the automatic calibration and detection of analog pointer instruments, which is of great research significance.

The key to the reading recognition of pointer instruments is pointer detection, and the existing pointer detection methods include the straight line fitting method,⁸ the frame difference method,^{9,10} the Hough straight line detection method,^{11,12} the central projection method.¹³ The pointer of the barometer tested in this paper has a medium length, and there is a mechanical device in the center of the dial, which makes the pointer disconnected from the center of the dial. Therefore, the straight line fitting and Hough straight line detection methods are not applicable. In addition, in the process of dial positioning, the Hough circle detection method requires several experiments to determine the appropriate parameters, which also affects the efficiency of the detection system. In the actual calibration system of this paper, each instrument has to go through 10 different pressure tests, and the control platform captures the value of each test and records the detection image of the instrument at the same time. Therefore, each meter corresponds to 10 images with the same background and different needle rotation angles. In view of the actual situation of the instrument, we propose a simple three-point circle finding method to realize the dial location, segmentation, and pointer centroid extraction. Then, the extracted pointer centroid is connected with the dial center to fit the pointer, and an improved angle method is proposed to realize the automatic identification of meter readings, which further improves the accuracy of automatic reading.

2 System Scheme

As shown in Fig. 1, the overall scheme of the system can be divided into six parts, including dial positioning, dial extraction, scale area extraction, scale calibration, pointer recognition, and reading recognition.

2.1 Dial Positioning

Based on the three-point circle finding method, the center of the dial ring and the dial radius are determined through the detected pointer information of 10 groups of test values, which are used for dial extraction, scale calibration, and reading identification.

2.2 Dial Extraction

According to the circle center and radius values obtained by dial positioning, appropriate dial cutting is carried out for scale area extraction and reading recognition.

2.3 Scale Area Extraction and Scale Calibration

The color image is separated by chromatic channels, and the dial scale area is extracted and fused, so as to realize dial scale extraction and centroid calibration.

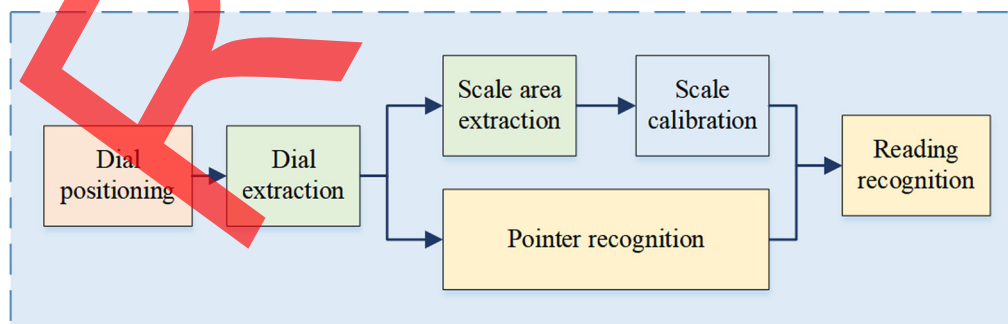


Fig. 1 Schematic diagram of the reading identification system for the pointer type barometer.

2.4 Pointer Recognition

The frame difference method is used to detect the pointer, and the binary image corresponding to the pointer of the test value is obtained, and the centroid of the pointer is obtained.

2.5 Reading Recognition

Multiple sets of reference scale values are selected according to the position of the centroid of the pointer, and the centroid of the pointer and the scale lines are connected to the center of the dial, and the improved angle method is adopted to realize reading recognition.

3 Dial Positioning and Extraction

3.1 Dial Positioning

Whether it is line detection or circle detection, the common methods are based on Hough transform. However, the parameter selection process of the Hough detection method is too cumbersome. It requires many experiments to determine the slope and intercept and also needs to construct the corresponding parameter space to determine the transformation formula. Although there is a device for instrument fixing on the calibration platform, it cannot ensure that the positions of all the tested instruments are exactly the same, so it is necessary to locate the dial to improve the accuracy. As shown in Fig. 2, each instrument has to undergo 10 groups of different pressure tests, and the pointer should also be positioned when reading the instrument. Considering the above actual situation, we adopt a simple three-point circle finding method to locate the dial. First, the centroids of the pointers corresponding to the test values are extracted through the fitting of the minimum circumscribed rectangle, then the optimal three points are selected to determine the center of the circle, and then the center of the dial of the pointer instrument is located.

According to the prior knowledge, the outer circle of the dial and the inner circle determined by the pointers are concentric circles. When the center of the dial is determined, the radius of the inner circle and the radius of the outer circle are proportional. Suppose that the coordinates of the three points that can form an approximate semicircle on the circle are $A(a_1, b_1)$, $B(a_2, b_2)$, and $C(a_3, b_3)$, the coordinates of the center O are (R_x, R_y) , and the radius of the circle is r , we can bring them into the equation of the circle:

$$(x - R_x)^2 + (y - R_y)^2 = r^2, \quad (1)$$

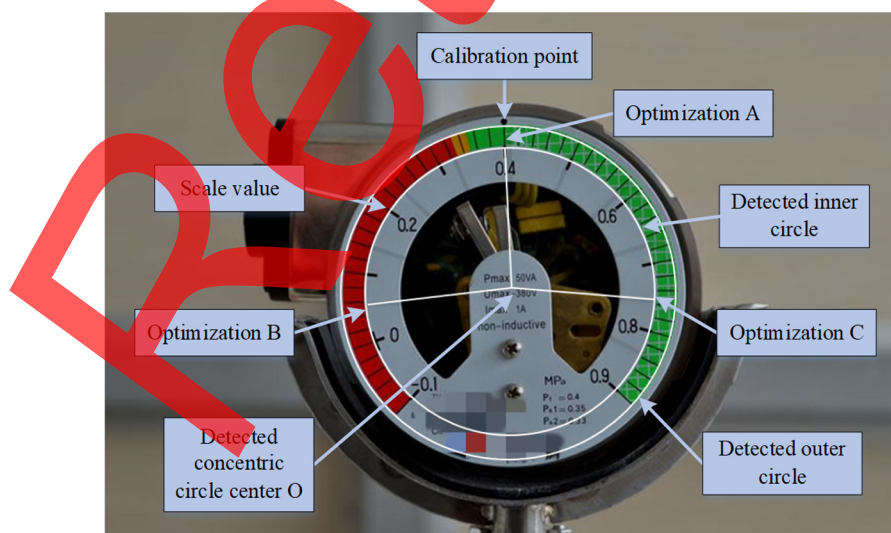


Fig. 2 Schematic diagram of dial positioning.

$$(a_1 - R_x)^2 + (b_1 - R_y)^2 = (a_2 - R_x)^2 + (b_2 - R_y)^2, \quad (2)$$

$$(a_1 - R_x)^2 + (b_1 - R_y)^2 = (a_3 - R_x)^2 + (b_3 - R_y)^2. \quad (3)$$

Through expansion and shift operations on Eq. (2), we can obtain

$$R_x = \frac{a_1^2 - a_2^2 + b_1^2 - b_2^2}{2a_1 - 2a_2} - \frac{(b_1 - b_2) \times R_y}{a_1 - a_2}, \quad (4)$$

$$u = \frac{a_1^2 - a_2^2 + b_1^2 - b_2^2}{2a_1 - 2a_2}, \quad (5)$$

$$k_1 = \frac{b_1 - b_2}{a_1 - a_2}, \quad (6)$$

$$R_x = u - k_1 \times R_y. \quad (7)$$

Through expansion and shift operations on Eq. (3), we can obtain

$$R_x = \frac{a_1^2 - a_3^2 + b_1^2 - b_3^2}{2a_1 - 2a_3} - \frac{(b_1 - b_3) \times R_y}{a_1 - a_3}, \quad (8)$$

$$v = \frac{a_1^2 - a_3^2 + b_1^2 - b_3^2}{2a_1 - 2a_3}, \quad (9)$$

$$k_2 = \frac{b_1 - b_3}{a_1 - a_3}, \quad (10)$$

$$R_x = v - k_2 \times R_y. \quad (11)$$

By bringing Eq. (11) into Eq. (7), we can obtain

$$R_y = \frac{u - v}{k_1 - k_2}, \quad (12)$$

$$R_x = v - \frac{(u - v) \times k_2}{k_1 - k_2}. \quad (13)$$

Based on the three-point circle finding method, the center and radius of a circle can be obtained by knowing any three points on the circle. In this paper, the three-frame difference method is used to extract the pointer by performing a difference operation on two adjacent frames of images in the video, and then the minimum circumscribed rectangle fitting method is used to locate the pointer centroid. The details are given in Sec. 5. For the 10 groups of detected pointers, we adopt three points *A*, *B*, and *C* as shown in Fig. 2 to locate the center of the circle. Figure 3 shows the pointer



Fig. 3 Schematic diagram of pointer extraction.

extraction results corresponding to 10 groups of air pressure test values. It can be seen that when the pointer corresponding to a test value falls on the scale lines or the numbers in the process of detection, these pointers cannot be completely detected, which leads to the incompleteness of the detected pointer. Even through the minimum circumscribed rectangle fitting, the real pointer cannot be completely extracted, so the obtained circumscribed rectangle centroid is not the real pointer centroid.

Because the size and shape of the 10 groups of extracted pointers are not exactly the same, when selecting the three points to locate the center of the circle, we can get the three extreme values (P_x^{\min} , P_x^{\max} and P_y^{\min}) from the abscissas and ordinates of the 10 centroids of the fitted pointers. Then, the corresponding coordinates of the three optimal points can be obtained, that is, the three points B , C , and A in Fig. 2. The main purpose of selecting positioning points in this way is to ensure that the three points form an approximate semicircle and make the fitted inner circle more accurate.

3.2 Dial Extraction

In the dial extraction process, to reduce the background interference, only the area containing the pointer and scales is cut out when preprocessing the collected images. Because there is no strong noise interference in the instrument images in our task, the maximum interclass variance method (a kind of global threshold methods) is adopted to segment the images through binarization. The principle of the maximum interclass variance method is to quantitatively reflect the uniformity of image gray distribution by variance. First, the gray values of the entire image are obtained, and the minimum to maximum gray value is used as the threshold for image segmentation. In this way, the gray values and the number of pixels of the target and background images after threshold segmentation can be obtained. Then, the interclass variances under different threshold conditions are calculated in turn, and the threshold corresponding to the maximum interclass variance is determined as the best threshold for binarization segmentation. An example of a binarized instrument image is shown in Fig. 4.

4 Scale Area Extraction and Scale Calibration

Figure 5 shows the flowchart of scale extraction. First, pixel-by-pixel comparison is made between two color images A and B with different pointer positions, and the maximum values are obtained. Since the background of the dial is the same and only the black pointer changes, the black pointer is replaced by the white dial background after comparing the pixel values of the two images point by point and only taking the maximum value between each pair of pixel values. Finally, a barometer image without a pointer can be obtained:

$$\text{Img} = \text{MAX}(A, B), \quad (14)$$

where $\text{Max}()$ represents the operation of pixel by pixel comparison of two images and taking the maximum pixel value. After obtaining the pointer-free barometer image, the dial scale area is

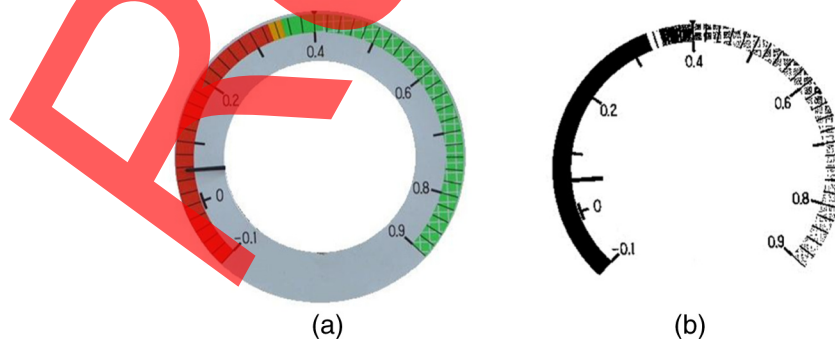


Fig. 4 An example of dial extraction: (a) the result of background removal and (b) the result of threshold segmentation.

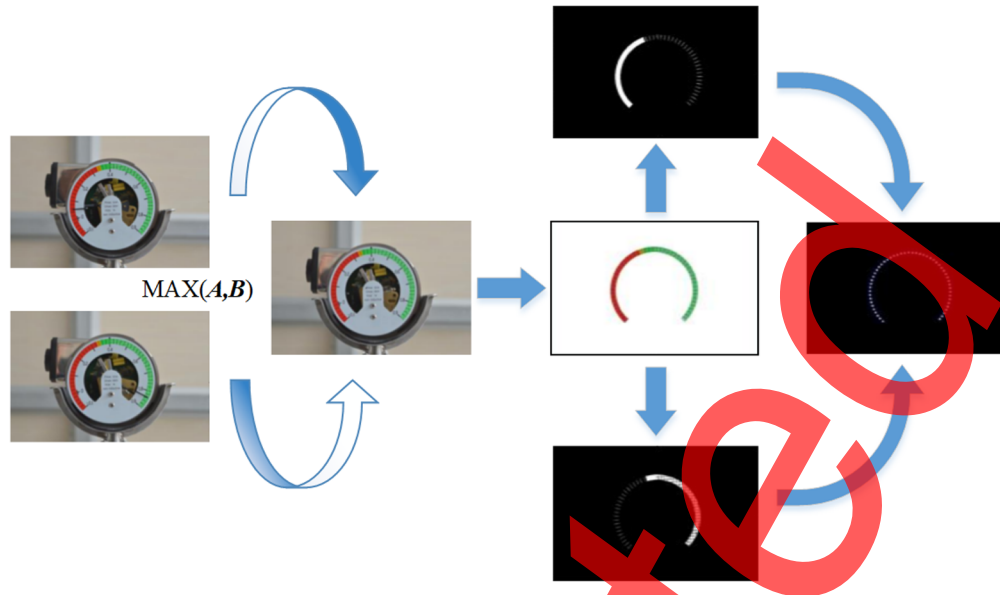


Fig. 5 Schematic diagram of scale extraction.

obtained by segmenting the dial image. Since the scale area is colored and the green scale part is mixed with some white stripes, we adopt the color channel extraction method to extract the scale area, and perform grayscale and binarization processing. In view of the slender scale lines of the instrument, appropriate expansion processing is also carried out to obtain two clear binarized images. Finally, an image with clear and complete scale lines is obtained through segmentation and splicing operations. To calibrate the scale values, we use the minimum external rectangle to fit each scale line and take the centroid of external rectangle as the centroid of each scale line and then establish the relationship between the centroid of each scale line and corresponding air pressure value as the basis for reading recognition.

5 Pointer Centroid Extraction

In this paper, the proposed reading recognition method is used for actual instrument calibration systems. Each instrument to be tested has to undergo 10 different air pressure tests, corresponding to 10 images with different pointer positions. To detect the pointer position, we use the three-frame difference method¹⁴ to perform differential operation on the instrument images corresponding to two adjacent tests to extract the position information of the pointer. The specific process is as follows: the instrument image corresponding to the current test value is taken as the reference frame, then the difference between the reference frame and the frames corresponding to the previous and subsequent test values is calculated, and the change of the pointer is finally detected. Assuming that the frame corresponding to the n 'th test value is I_n , and the previous and subsequent frames are I_{n-1} and I_{n+1} , then the difference can be obtained as

$$D_1 = I_{n-1} - I_n, \quad (15)$$

$$D_2 = I_{n+1} - I_n. \quad (16)$$

Then, the binarized image of the pointer can be obtained through binarizing the difference result and performing logic AND operation:¹⁵

$$D_n = M(D_1) \wedge M(D_2), \quad (17)$$

where $M()$ represents the binarization processing. Then, the minimum circumscribed rectangle fitting is performed on the pointer region obtained after binarization, and the centroid of the minimum circumscribed rectangle can be obtained and used as the pointer centroid:

$$J_n = W(D_n), \tag{18}$$

where $W()$ represents the fitting operation of minimum circumscribed rectangle.

6 Reading Identification

After the centroid of the pointer is obtained, the real pointer can be represented by the connecting line OP between the dial center O and the pointer centroid P . Since each small scale in the dial may not be completely detected, we only select 11 calibration scales $(-0.1, 0, 0.1, 0.2, 0.3, 0.4, 0.5, 0.6, 0.7, 0.8, 0.9)$ with longer scale lines as the calibration scale points K_m , where $m \in \{1, \dots, 11\}$. In the actual test, the dial pointer must be between the point K_m and K_{m+1} . Therefore, there are m scale values on the left side of the pointer and $11-m$ scale values on the right side of the pointer. Taking any calibration scale value p_i from the m calibration scale values on the left side of the pointer, and taking any calibration scale value p_j from the $11-m$ calibration scale values on the right side of the pointer, the reading result corresponding to OP can be calculated according to the angular deviation between the line OP and the two lines connecting the two calibration scales and the point O . Assuming that the point M and point N correspond to the two selected calibration pressure scale values p_i and p_j , it can be determined that the reading result of pointer OP is within the range of (p_i, p_j) . According to the known coordinates of the four points O, P, M , and N , the angle values θ and ω of $\angle MON$ and $\angle MOP$ can be obtained using the cosine formula. When $p_j > p_i$, the reading result corresponding to OP is

$$p = \frac{\omega}{\theta} (p_j - p_i) + p_i. \tag{19}$$

This is only the reading recognition result obtained by a pair of calibration scales. As mentioned above, from the m calibration scale values on the left side of the pointer and the $11-m$ calibration scale values on the right side, we can get $m \times (11-m)$ calibration scale combinations and obtain $m \times (11-m)$ reading results. To improve the reliability of reading recognition, the average of these reading results can be taken as the final reading recognition result:

$$\bar{p} = \frac{1}{m \times (11-m)} \sum_{u=1}^{m \times (11-m)} p_u. \tag{20}$$

As shown in Fig. 6, the area where the pointer OP is located is between the scales of 0 and 0.1. Two calibration scale values can be obtained on the left side of the pointer, and 9 calibration

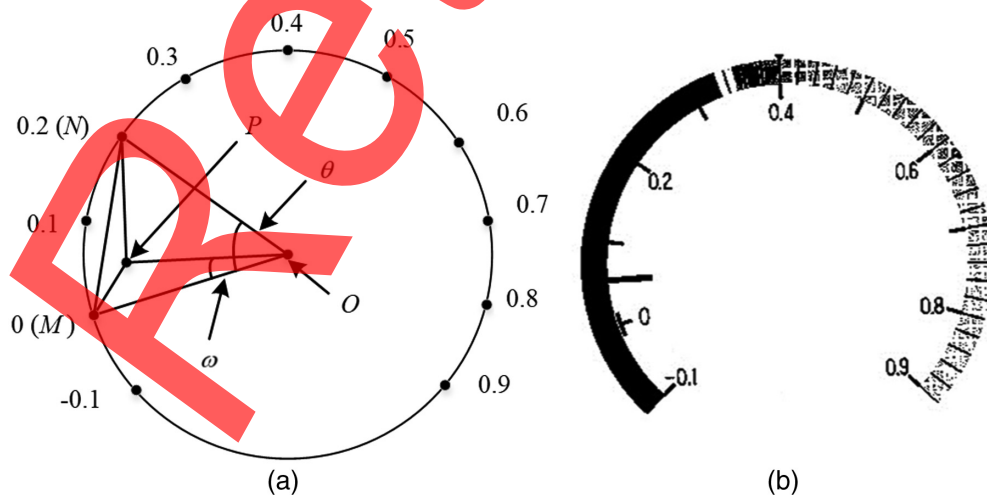


Fig. 6 Improved angle method for reading recognition: (a) principle of angle method and (b) calibration scales for reading recognition.

scale values can be obtained on the right side of the pointer. The angle method described above can get 18 reading results, and a more accurate meter reading can be obtained by averaging these 18 results.

Compared with the traditional angle method, the improved angle method not only avoids quadrant judgment and coordinate conversion but also overcomes the problem of relying too much on the starting scale line. Therefore, the improved angle method proposed in this paper has universal applicability. Moreover, this method calculates readings based on multiple sets of calibration scales, which avoids the error caused by unclear scale extraction to a certain extent, and improves the accuracy while facilitating scale extraction.

7 Experimental Results

Finally, we implemented and tested the overall scheme through Visual Studio 2019. The computer used for the test was configured with a 3.2 GHZ octa-core CPU and a 16 GB RAM. First, the three-point circle finding method was tested, and the time consumption results are shown in Table 1. The detection time consumption is the average time consumption of 10 runs of the program. It can be seen that the time consumption of the method used in this experiment is basically the same as that of Hough circle detection method, but the difficulty of parameter selection of Hough circle detection is avoided. At the same time, this three-point circle finding method can more accurately fit the center coordinates, and the detection results of the center coordinates are shown in Table 2. Moreover, this method can obtain the coordinates of the centroid of the pointer while detecting the circle center, which is more efficient than the Hough circle detection method as a whole.

To improve the reliability of performance comparison, we organized 10 volunteers to perform manual reading identification, and at the same time performed the tail-cutting mean operation on the results of these 10 readings, and used the mean value as the benchmark reference for the calculation of reading identification accuracy. Table 3 shows the reading recognition results based on the manual method, the traditional angle method, and the improved angle method, as well as the absolute and relative errors between automatic recognition results and manual reading results. It can be seen that the efficiency of the improved angle method is better than that of the traditional angle method to a certain extent. The defect of the traditional angle method is that the reading error increases with the increase of the angle, so the reading value becomes inaccurate as the pressure value increases, and the overall value is too large. The improved angle method proposed in this paper can obtain higher accuracy.

Table 1 Time consumption of the three-point circle finding method and the Hough circle detection method (unit: s).

Method	Time
Three-point circle finding method	1.014
Hough circle detection method	0.884

Table 2 Center coordinates obtained by the three-point circle finding method and the Hough circle detection method.

Method	Coordinates
Actual calibration	(405,280)
Three-point circle finding method	(409,280)
Hough circle detection method	(407,281)

Table 3 Reading recognition results based on different methods (unit: MPa).

No.	Manual method	Traditional angle method	Absolute error	Relative error (%)	Improved angle method	Absolute error	Relative error (%)
1	0.055	0.056	-0.001	1.79	0.055	0.000	0.00
2	0.140	0.141	-0.001	0.71	0.140	0.000	0.00
3	0.235	0.237	-0.002	0.84	0.235	0.000	0.00
4	0.324	0.325	-0.001	0.31	0.323	0.001	0.31
5	0.405	0.409	-0.004	0.98	0.406	-0.001	0.25
6	0.500	0.500	0.000	0.00	0.498	0.002	0.40
7	0.585	0.548	0.037	6.75	0.584	0.001	0.17
8	0.670	0.672	-0.002	0.30	0.670	0.000	0.00
9	0.760	0.775	-0.015	1.94	0.759	0.001	0.13
10	0.835	0.835	0.000	0.00	0.835	0.000	0.00

8 Conclusions

Aiming at the computer vision-based automatic calibration system of a pointer barometer, we adopt a simple three-point circle finding method to locate the meter and propose an improved angle method for automatic reading recognition. The experimental results show that the three-point circle finding method can detect the center of the circle efficiently, which provides the basic condition for the automatic reading recognition based on the improved angle method. The improved angle method is generally applicable and has the advantages of high precision, high real-time performance, and high reliability. The overall reading recognition scheme in this paper has strong pertinence and practicability and can provide reference for relevant practical applications.

Acknowledgments

This work was supported by the National Natural Science Foundation of China under Grant Nos. 61702462, 62072416, 61873246, and 61771432, the Scientific and Technological Project of Henan Province under Grant Nos. 222102210010 and 192102210108, and the Research and Practice Project of Higher Education Teaching Reform in Henan Province under Grant Nos. 2019SJGLX320 and 2019SJGLX020. The author(s) declared no potential conflicts of interest with respect to the research, authorship, and/or publication of this paper. This paper does not contain any studies with human participants or animals performed by any of the authors.

References

1. G. Xiong, W. Xiao, and X. Wang, "Overview of the detection and recognition methods of pointer meters based on vision," *Sens. Microsyst.* **39**(12), 1–3 +9 (2020).
2. E. Tunca et al., "Determining the pointer positions of aircraft analog indicators using deep learning," *Aircr. Eng. Aerosp. Technol.* **94**(3), 372–379 (2021).
3. W. Ding and B. Zhang, "Detection and recognition method for pointer-type meter based on deep learning," in *IEEE 3rd Int. Conf. Civil Aviat. Safety and Inf. Technol.*, IEEE, pp. 1088–1091 (2021).
4. Z. Zhang et al., "Pointer meter reading recognition based on machine vision," *Control Eng.* **27**(3), 581–586 (2020).
5. L. Wang et al., "Computer vision based automatic recognition of pointer instruments: data set optimization and reading," *Entropy* **23**(3), 272 (2021).

6. F. Kong et al., "End-to-end multispectral image compression framework based on adaptive multiscale feature extraction," *J. Electron. Imaging* **30**(1), 013010 (2021).
7. C. Huang, "Particle swarm optimization in image processing of power flow learning distribution," *Discov. Internet Things* **1**, 12 (2021).
8. D. Uhlig and M. Heizmann, "A calibration method for the generalized imaging model with uncertain calibration target coordinates," in *Proc. Asian Conf. Comput. Vision*, pp. 541–559 (2020).
9. D. K. Jain et al., "An efficient and adaptable multimedia system for converting PAL to VGA in real-time video processing," *J. Real Time Image Process.* **17**(6), 2113–2125 (2020).
10. S. S. Sengar and S. Mukhopadhyay, "Moving object detection using statistical background subtraction in wavelet compressed domain," *Multimedia Tools Appl.* **79**(9), 5919–5940 (2020).
11. J. Huang et al., "An automatic analog instrument reading system using computer vision and inspection robot," *IEEE Trans. Instrum. Meas.* **69**(9), 6322–6335 (2020).
12. D. K. Jain et al., "Deep neural learning techniques with long short-term memory for gesture recognition," *Neural Comput. Appl.* **32**(20), 16073–16089 (2020).
13. C. Wang et al., "A novel unsupervised dead-value detection method for monitoring indicators in data center," in *Int. Conf. High Perform. Big Data and Intell. Syst.*, IEEE, pp. 1–6 (2020).
14. K. S. Chandrasekar and P. Geetha, "Multiple objects tracking by a highly decisive three-frame differencing-combined-background subtraction method with GMPFM-GMPHD filters and VGG16-LSTM classifier," *J. Vis. Commun. Image Represent.* **72**, 102905 (2020).
15. N. Srivastav et al., "Hybrid object detection using improved three frame differencing and background subtraction," in *7th Int. Conf. Cloud Comput., Data Sci. and Eng.-Confluence*, IEEE, pp. 613–617 (2017).

Zuhe Li is an associate professor at Zhengzhou University of Light Industry. He received his BS degree in electronic information science and technology from Zhengzhou University of Light Industry in 2004, his MS degree in communication and information system from Huazhong University of Science and Technology in 2008, and his PhD in information and communication engineering from Northwestern Polytechnical University in 2017. His current research interests include computer vision, sentiment analysis, and machine learning.

Yuan Yu is a teaching assistant at Zhengzhou University of Light Industry. He received his degree from Nanyang Normal University, Nanyang, China, in 2013. He is currently working toward his master's degree in the School of Computer and Communication Engineering, Zhengzhou University of Light Industry. His current research interests include computer vision, sentiment analysis, and machine learning.

Baohua Jin received his master's degree in computer science and technology from Huazhong University of Science and Technology, Wuhan, China, in 2003. He is a professor in the School of Computer and Communication Engineering at Zhengzhou University of Light Industry, Zhengzhou, China. His current research topics include computer engineering and applications, information communication, and processing.

Yuhao Cui received his BE degree from Zhengzhou University of Light Industry, Zhengzhou, China, in 2021. He is currently working toward his master's degree in the School of Computer and Communication Engineering, Zhengzhou University of Light Industry. His current research interests include computer vision and machine learning.